Food Chemistry 374 (2022) 131558

Contents lists available at ScienceDirect

Food Chemistry

journal homepage: www.elsevier.com/locate/foodchem

Transcriptome sequencing and metabolomics analyses provide insights into the flavonoid biosynthesis in *Torreya grandis* kernels

Feicui Zhang [a,1], Zhenmin Ma [a,1], Yan Qiao [b], Zhanqi Wang [c], Wenchao Chen [a], Shan Zheng [a], Chenliang Yu [a], Lili Song [a,*], Heqiang Lou [a,*], Jiasheng Wu [a,*]

[a] State Key Laboratory of Subtropical Silviculture, Zhejiang A&F University, Hangzhou, Zhejiang 311300, China
[b] College of Agriculture and Forestry, Longdong University, Qingyang 745000, China
[c] Key Laboratory of Vector Biology and Pathogen Control of Zhejiang Province, College of Life Sciences, Huzhou University, Huzhou 313000, China

ARTICLE INFO

Keywords:
Antioxidant activity
Flavonoid biosynthetic pathway
Transcriptome
Metabolomics
Torreya grandis

ABSTRACT

The kernel of *Torreya grandis* (*T. grandis*) is a rare nut with a variety of bioactive compounds. Flavonoids are a very important class of bioactive compounds with high antioxidant activity in *T. grandis* kernels. However, the flavonoid compositions which mainly contribute to antioxidant capacity and the molecular basis of flavonoid biosynthesis in *T. grandis* remain unclear. Here, transcriptome sequencing and metabolomics analysis for kernels were performed. In total, 124 flavonoids were identified. Among them, 9 flavonoids were highly correlated with antioxidant activity. Furthermore, unigenes encoding CHS, DFR and ANS showed significant correlation with the 9 flavonoids. Transient overexpression of *TgDFR1* in tobacco leaves resulted in increased antioxidant activity. Moreover, several transcription factors from MYB, bHLH and bZIP families were identified by co-expression assay, suggesting that they may regulate flavonoid biosynthesis. Our findings provide a molecular basis and new insights into the flavonoid biosynthesis in *T. grandis* kernels.

1. Introduction

As dietary antioxidants, flavonoids are a class of secondary metabolites occurring ubiquitously in food plants, with over 6000 individual compounds known (Harborne & Williams, 2000). The basic flavonoid structure is a C6-C3-C6 system, the three rings are labeled A, C and B. The level of oxidation and pattern of substitution of the C ring divide flavonoids into six categories including flavones, flavonols, flavanones, proanthocyanidins, isoflavones and anthocyanins, while the pattern of substitution of the A and B rings determine individual compounds within a class (Lepiniec et al., 2006). Due to the chemical structure, most flavonoids exhibit strong antioxidant activity (Li et al., 2008). In human beings, flavonoids play important roles in protecting against liver injury, oxidative stress, vascular disease, the occurrence of diabetes and hypertension, and cancer (Giménez-Bastida & Zieliński, 2015; Hu et al., 2015; Hu et al., 2016; Lee et al., 2013). There are several antioxidant mechanisms flavonoids were found. Flavonoids stabilize the reactive oxygen species by reacting with the reactive compound of the radical. Because of the high reactivity of the hydroxyl group of the flavonoids, radicals are made inactive. Some flavonoids, such as quercetin and silibin, inhibit xanthine oxidase activity, thereby resulting in decreased oxidative injury. Several flavonoids, including quercetin, result in a reduction in ischemia–reperfusion injury by interfering with inducible nitric-oxide synthase activity. Some flavonoids can inhibit degranulation of neutrophils without affecting superoxide production. In addition, some flavonoids attenuated the free radicals-induced damage on antioxidant enzymes by scavenging the radicals and flavonoids bound with the antioxidant enzymes and caused direct activation of these enzymes, where any of these mechanisms will result in increased activity of the antioxidant enzyme (Nijveldt et al., 2001).

The flavonoid biosynthesis pathway is initiated by the condensation of one molecule of 4-coumaroyl-CoA with three molecules of malonyl-CoA by the chalcone synthase (CHS) enzyme. Then the involvement of chalcone isomerase (CHI), flavanone 3-hydroxylase (F3H), dihydroflavonol 4-reductase (DFR), and anthocyanidin synthase (ANS) lead to the synthesis of anthocyanidin pigments. Flavone synthase (FNS) and Isoflavone synthase (IFS) produces flavones and isoflavones. Flavonol synthase (FLS) catalysis dihydroflavonols to flavonols, while

* Corresponding authors.
E-mail addresses: lilisong@zafu.edu.cn (L. Song), 20170030@zafu.edu.cn (H. Lou), wujs@zafu.edu.cn (J. Wu).
[1] These authors contributed equally to this work.

https://doi.org/10.1016/j.foodchem.2021.131558
Received 31 August 2021; Received in revised form 4 November 2021; Accepted 5 November 2021
Available online 8 November 2021

leucoanthocyanidin reductase (LAR) and anthocyanidin reductase (ANR) synthesize *trans*- or *cis*- flavan-3-ols, the precursors of proanthocyanidin (PA) polymers. Numerous studies have indicated that the expression of the genes involved in the flavonoid biosynthetic pathway is controlled by distinct mechanisms in a tissue- or species-specific manner. In vegetative tissues, anthocyanin biosynthesis is regulated by different MYB–bHLH–WDR (MBW) complexes involving PAP1/MYB75 and PAP2/MYB90, in combination with GL3/bHLH00, EGL3/bHLH002, TT8/bHLH042 and TTG1 (Appelhagen et al., 2011). In seeds, TT2/MYB123, TT8 and TTG1 are the main PA biosynthesis regulators. In *Arabidopsis thaliana*, the TT2–TT8–TTG1 complex plays the major role in the development of seeds by regulating *DFR*, *LDOX*, *BAN*, *TT19*, *TT12* and *AHA10* in all the PA accumulating cells (i.e. micropyle, chalaza and endothelium), whereas the MYB5–TT8–TTG1 complex is only active in the endothelium where it regulates *DFR*, *LDOX* and *TT12* expression (Xu et al., 2014).

T. grandis Fort. ex Lindl is an evergreen tree belonging to the Taxaceae family, of which *T. grandis* cv. Merrillii is the only grafted and thoroughbred species. As one of the rare nuts and the important traditional medicine, the kernels of *T. grandis* are rich in tocopherols, unsaturated fatty acids and flavonoids (Dai et al., 2007; Ding et al., 2020; He et al., 2016; Lou et al., 2019). Studies have identified that the kernels or leaves of *T. grandis* have multiple biological properties, such as anti-inflammatory (Saeed et al., 2010), antioxidative (Cui et al., 2018), and anthelmintic activity (Liu et al., 2018). These studies suggest both high nutritional and medicinal value of *T. grandis* seeds. However, the compositions, biosynthesis pathway and transcriptional regulation of flavonoid in *T. grandis* seeds remain completely unknown.

In this study, we took advantage of metabolite profiling and transcriptomic analysis to investigate flavonoid biosynthesis in developing *T. grandis* kernels. In total, 124 flavonoids were identified including 53 flavones, 31 flavonols, 3 proanthocyanidins, 20 flavanones, 9 isoflavones and 8 anthocyanins, among which, 9 flavonoids were highly correlated with antioxidant activity. Furthermore, the unigenes of flavonoid biosynthesis pathway were also identified. The key genes controlling the 9 flavonoids biosynthesis and antioxidant ability of *T. grandis* kernels were revealed by Pearson correlation analysis. The function of *TgDFR1* in improving antioxidant activity was confirmed by transient overexpression of it in tobacco leaves. The data in this study largely expanded our knowledge of flavonoid biosynthesis in developing *T. grandis* kernels at both metabolic and molecular levels, and also provided valuable information for the further development of new health products based on *T. grandis*.

2. Material and methods

2.1. Plant material

Three *T. grandis* cv. 'Merrillii' grafting trees planted at Dongqiao Town, Fuyang City, Zhejiang Province were used in this study. The seeds of *T. grandis* were harvested 450, 480 and 510 days after pollination, respectively (July to September 2018, marked as Stage 1, Stage 2 and Stage 3, respectively). After collection, the arils and seed coats were removed and the remaining kernels were immediately frozen in liquid nitrogen and stored at −80 °C until use. In each biological replicate, 10 kernels were ground into powder together in liquid nitrogen, and then divided into three parts, which were used for RNA sequencing, metabolite profiling and physiological assay, respectively. Three biological replicates were used for each experiment. About 0.5 g kernels were ground with liquid nitrogen, then added 3 mL methanol, drew supernatant after ultrasound (800 W) for one hour. The supernatant were used for total flavonoid content, DPPH and FRAP determination.

2.2. Total flavonoid content determination

The total flavonoid content was determined according to the method of Bonvehí et al with modifications (Bonvehí et al., 2001). Briefly, 0.5 mL solution of *T. grandis* kernel in methanol was separately mixed with 0.1 mL of 2% aluminum chloride, 1.5 mL of methanol, 0.1 mL of 1 M potassium acetate, and 2.8 mL of distilled water. The absorbance was measured at 415 nm using a spectrophotometer at room temperature. The total flavonoid content was expressed as rutin equivalents in milligrams per gram fresh weight of *T. grandis* kernel. Three biological replicates were performed.

2.3. DPPH radical scavenging activity determination

DPPH radical scavenging activity was analyzed by the method of Lu et al with modifications (Lu et al., 2010). The methanol extracts (0.1 mL) of *T. grandis* kernel or flavonoid standards (spiraeoside, chrysoeriol, hesperetin, naringenin and rutin) with the same content to total flavonoids of kernels in the stage 2 in were reacted with 7.9 mL of 0.03 g/L DPPH (2, 2-diphenyl-1-picrylhydrazyl) ethanol solution at room temperature. The absorbance was measured at 517 nm against an ethanol blank after 30 min of reaction in the dark at room temperature. The scavenging activity was expressed as (SA, %) = $100\times(1 - As/Ac)$, where Ac is the absorbance of 7.9 mL DPPH with 0.1 mL methanol and As is the absorbance of 7.9 mL DPPH added to 0.1 mL sample. Three biological replicates were performed.

2.4. FRAP assay

FRAP assay was used based upon the methodology described previously (Benzie & Strain, 1996). FRAP reagent was freshly prepared to comprise 1 mM 2,4,6-tripyridyl-2-triazine (TPTZ) and 2 mM ferric chloride in 0.25 M sodium acetate (pH 3.6), besides, TPTZ was dissolved in 40 mM HCl. A 0.1 mL aliquot of *T. grandis* kernel was added to 0.9 mL of FRAP reagent and mixed. After standing at room temperature (25 °C) for 4 min, absorbance was determined at 593 nm. The standard curve (100–600 mM ferrous ion) was produced by the addition of freshly prepared ammonium ferrous sulphate to FRAP reagent. FRAP values are presented as micromolar ferrous ion (ferric reducing power) of a 100% extracts, and three biological replicates were performed.

2.5. RNA extraction and transcriptome analysis

Total RNA was isolated from the kernels of *T. grandis* using the RNAprep Pure Plant Kit (DP441, Tiangen), mRNA was purified using poly(A) selection, and chemically fragmented and converted into single-stranded cDNA using random hexamer priming. Next, the second strand was generated to create double-stranded cDNA. Then, an A base was added to the blunt ends to make them ready for the ligation of sequencing adapters. After size selection of the ligation products using AMPure XP beads, the ligated cDNA fragments that contained adapter sequences were enhanced via PCR using adapter-specific primers. After diluting the library to 1.5 ng/μL, the insertional fragments of the library were detected by Agilent 2100 Bioanalyzer. Three biological replicates were used for transcriptome sequencing.

After filtering the original sequencing data, high-quality reads were obtained and the transcriptome of the species was obtained by splicing (Trinity, 2.6.6). Then we compared the high-quality reads with the spliced transcriptome (Bowtie2, 2.3.4.1), calculated the gene expression using RSEM (1.2.28), and annotated and enriched the differentially expressed genes using DESeq2 (1.20.0) and clusterProfiler (3.8.1). The false discovery rate (FDR) was obtained by using the Benjamin–Hochberg method to correct the hypothesis test probability (P value). The screening criteria for differential gene were $|\log2FC| \geq 1$ and FDR < 0.05. BLAST software was used to compare cDNA or protein sequences to the KEGG database to obtain the KO number of the genes, and then, the KEGG pathways for the genes were determined. The screening criterion for the KEGG enrichment analysis was a corrected *P*-value <0.05.

2.6. Metabolite extraction and profiling

Extraction and analysis of metabolites were carried out by the Metware Biotechnology Co. Ltd. (Wuhan, China). Three biological replicates were used. The prepared samples were freeze-dried and then were ground for 1.5 min at 30 Hz using a mixer mill (MM400, Retsch) with a zirconia bead. 100 mg of each sample was extracted in 1.0 mL 70% aqueous methanol overnight at 4 °C. During the extraction process, the sample was vortexed three times for improving extraction rate. Following centrifugation at 10,000*g* for 10 min, all the supernatants were pooled and filtered with a membrane (SCAA-104, 0.22 mm pore size; ANPEL, Shanghai, China) before LC-MS/MS analysis. An LC-ESI-MS/MS system (UPLC, Shim-pack UFLC SHIMADZU CBM30A system, www.shimadzu.com.cn/; MS/MS, Applied Biosystems 6500 Q TRAP, www.appliedbiosystems.com.cn/) was used to analyze the extracts. The UPLC conditions were as follows: Column, Waters ACQUITY UPLC HSS T3 C18 (1.8 μm, 2.1 mm*100 mm); solvent system, water (0.04% acetic acid):acetonitrile (0.04% acetic acid); gradient program,95:5V/V at 0 min, 5:95 v/v at 11.0 min, 5:95 v/v at 12.0 min, 95:5 v/v at 12.1 min, 95:5 V/V at 15.0 min; flow rate, 0.40 mL/min; temperature, 40 °C; injection volume, 2 μl. The effluent was connected to an ESI-triple quadrupole-linear ion trap (Q TRAP)-MS. LIT and triple quadrupole (QQQ) scans were acquired on a triple quadrupole-linear ion trap mass spectrometer (Q TRAP), API 6500 Q TRAP LC/MS/MS System, equipped with an ESI Turbo Ion-Spray interface, operating in a positive ion mode and controlled by Analyst 1.6.3 software (AB Sciex). The ESI source operation parameters were as follows: ion source, turbo spray; source temperature 500 °C; ion spray voltage (IS) 5500 V; ion source gas I (GSI), gas II (GSII), curtain gas (CUR) were set at 55, 60, and 25.0 psi, respectively; the collision gas (CAD) was high. Instrument tuning and mass calibration were performed with 10 and 100 μmol/L polypropylene glycol solutions in QQQ and LIT modes, respectively. QQQ scans were acquired as MRM experiments with collision gas (nitrogen) set to 5 psi. A scheduled multiple reactions monitoring method was used to quantify metabolites. To generate maximal signal, collision energy (CE) and de-clustering potential (DP) were optimized for each precursor-product ion (Q1-Q3) transition. A specific set of MRM transitions was monitored for each period on the basis of the eluted metabolites.

2.7. MS data and statistical analysis

Using a self-built database, the Metware MS2 spectral tag (MS2T) library (Wuhan Metware Biotechnology Co., Ltd., Wuhan, China; http://www.metware.cn), and the public database of metabolite information, the isotope signals, repeated signals containing K^+, Na^+ and NH_4^+ ions, and the repeated signals of fragment ions with higher molecular weights were removed prior to the analysis. Metabolite quantification was performed by a MRM analysis using the triple quadrupole MS. After obtaining the MS data of metabolites from different samples, the peak areas of all the mass spectral peaks were integrated, and peaks representing the same metabolite in different samples were integrated and corrected.

The metabolite content data were normalized with the range method using R software (www.r-project.org). Cluster analysis was used to analyze the accumulation patterns of metabolites among different samples. Fold change (FC) and variable importance in projection (VIP) value of orthogonal partial least squares discriminant analysis (OPLS-DA) model were used to screen the differential metabolites. Screening criteria were as follows: when $FC > 2$ or $FC < 0.5$ and $VIP \geq 1$ occurred, the difference was significant. The Kyoto Encyclopedia of Genes and Genomes (KEGG) pathway database was used to annotate the different metabolites. The web-based sever Metabolite Sets Enrichment Analysis (http://www.msea.ca) was used for the pathway enrichment analysis. A *P*-value <0.05 was considered to indicate significant enrichment.

2.8. Vector construction and transient expression of TgDFR1 and TgDFR2 in tobacco leaves

The cDNA libraries of *T. grandis* were prepared using SuperScript II reverse transcriptase (Vazyme) with random primers. *TgDFR1* and *TgDFR2* were amplifiied from cDNA using Phanta Max Super-Fidelity DNA polymerase (Vazyme) and cloned into a 35S::GFP (modified from pCAMBIA1300) for sequencing and introducing into *Agrobacterium tumefaciens*.

The transient gene expression analysis of *TgDFR1* and *TgDFR2* in *N. benthamiana* was performed according to a previous study (Lou et al., 2019). All constructs were transformed into *Agrobacterium tumefaciens* GV3101 strain. Agrobacteria was grown overnight in LB media and brought to OD_{600} of 0.8 in injection solution. After 3 days injection, green fluorescent protein (GFP) fluorescence was observed via confocal laser scanning microscopy (LSM510, Karl Zeiss).

Tissues used for DPPH radical scavenging activity and FRAP analyses were sampled from leaves after injection for 7 days. About 0.4 g injected leaves were ground with liquid nitrogen, then added 4 mL methanol, drew supernatant after ultrasound for one hour. The supernatant was used for DPPH and FRAP determination. Three biological replicates were used.

2.9. Quantitative real-time PCR (qRT-PCR)

Total RNA used for qRT-PCR was extracted using RNAprep Pure Plant Kit (DP441, Tiangen). Then the RNA was reverse transcribed to the first-strand cDNA using the Reverse Transcription Kit (PrimeScript™ RT Master Mix, Takara). The qRT-PCR was performed with a C1000 Touch™ Thermal Cycler system (Bio-Rad) and the ChamQ SYBR qPCR Master Mix kit (Vazyme). Relative expression level was calculated according to the $2^{-\triangle\triangle Ct}$ method. The actin gene was used as a reference gene. Ct represents the PCR cycle number at which the amount of target reaches a fixed threshold. Three biological and technical replications were performed.

2.10. Identification of candidate transcription factors by co-expression assay

To search for the transcription factors that were coexpressed with candidate genes, Pearson's correlation analysis between the expression level of all the transcripts annotated as transcription factors and candidate genes was performed using SPSS, version 16.0 (SPSS, Inc., Chicago, IL, U.S.A.). The transcription factors with Pearson's correlation coefficients $\geq$0.9 were selected for further analysis.

2.11. Statistical and sequence analyses

Correlations among data were calculated by Pearson's correlation coefficients (*r*), using SPSS, version 16.0 (SPSS, Inc., Chicago, IL, U.S.A.). Significant differences were determined using Duncan's new multiple range test at $p < 0.05$. Phylogenetic analysis was done using a bootstrap neighbor-joining evolutionary tree by MEGA 7.0 software with 1000 bootstrap replicates. Amino acid sequence alignment was conducted with DNAMAN software (version 9).

3. Results

3.1. Differentially accumulated metabolites (DAMs) of T. grandis kernels in the three maturation stages

The changes in metabolites during *T. grandis* kernel maturation were studied using a UPLC-MS/MS analysis. A total of 612 metabolites were detected in the metabolic analysis on the basis of widely targeted metabolomics (Table S1). A heatmap was used to show the DAMs between the three maturation stages (Fig. 1A). To analyze the specific

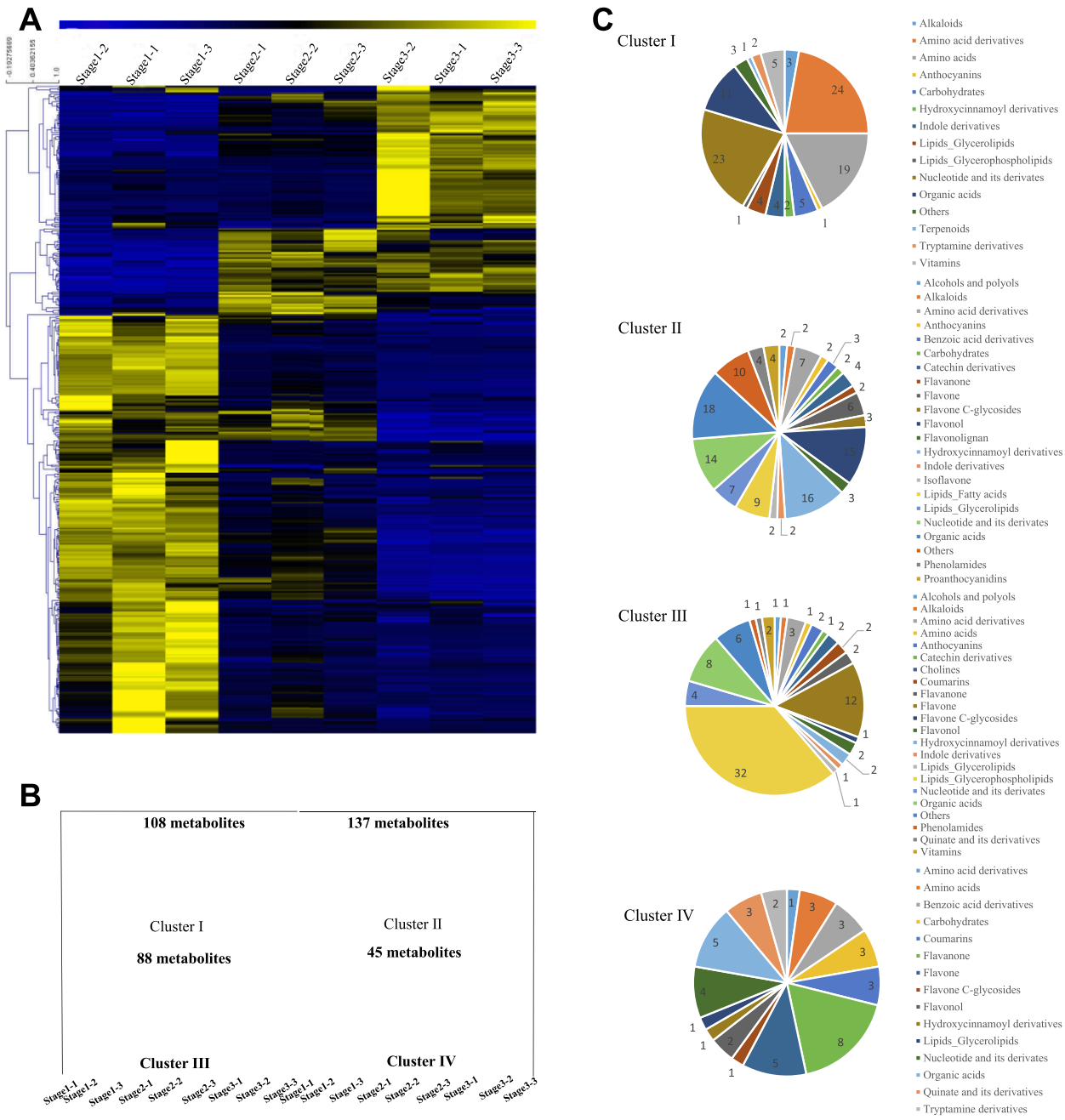

Fig. 1. The variations in the metabolites among three kernel development phases. (A) A heatmap of the relative amounts of DAMs from the three kernel development phases. (B) Clustering of the DAMs into four Clusters. (C) MeV cluster analysis of DAMs from the widly targeted metabolomic profiles.

metabolites accumulated during kernel development, all DAMs were grouped into four clusters (I–IV) (Fig. 1B). DAMs belonging to Cluster I and Cluster II predominantly accumulated in the stage 1; DAMs grouped into Cluster III were highly accumulated in the stage 3; DAMs in Cluster IV were abundant in the stage 2 (Fig. 1B). In Cluster I, the major DAMs were amino acid derivative, nucleotide, and amino acids; all the predominant DAMs in Cluster II, Cluster III and Cluster IV were flavonoids (Fig. 1C), suggesting that flavonoids were predominantly changed among the three maturation stages.

3.2. Total flavonoid content, DPPH radical scavenging activity and FRAP

The seed development of *T. grandis* can be divided into four stages: slow-growing stage, expansion stage, filling stage and mature stage. Among them, the filling stage and mature stage are the key periods for material transformation and accumulation. Stage 1 is the early filling stage, stage 2 is the late filling stage, and stage 3 is the mature stage. Total flavonoid content, DPPH radical scavenging activity and FRAP were further determined in these stages.

During the period of the Stage 1 to Stage 3, flavonoids content increased from 0.423 mg/g to 8.29 mg/g. (Fig. 2A). DPPH radical scavenging activity and FRAP both represented total antioxidant activities based on different measurement methods. Both DPPH radical scavenging activity and FRAP were increased at stage 2 and decreased at Stage 3 (Fig. 2B and C), however, their changing trend is not consistent with that of total flavonoid content.

3.3. Transcriptome analysis of the developmental kernels of T. grandis

To further investigate the potential molecular mechanisms of

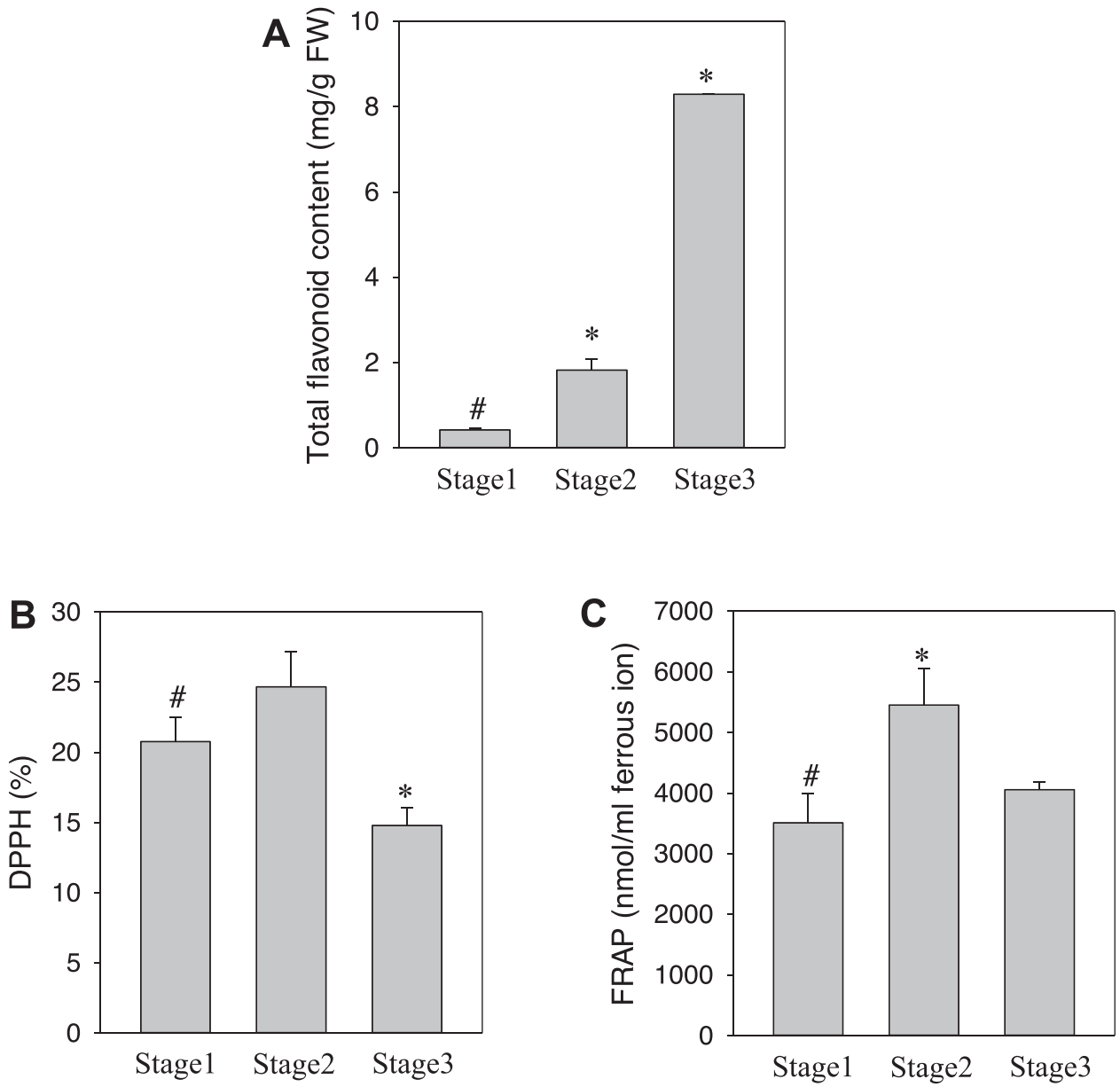

Fig. 2. Changes in total flavonoid content (A), DPPH radical scavenging activity (B) and FRAP values (C). FW, fresh weight. Data are means ± SEM ($n = 3$), asterisk (*) means $p < 0.05$.

flavonoid biosynthesis in the development of *T. grandis* kernels, 9 samples were used for RNA-seq analysis. All of the transcriptional data were deposited in the NCBI Sequence Read Archive (BioProject: PRJNA672806). PCA showed a low variability among biological repeats, which indicated that there was a high correlation between repetitions (Fig. 3A). The 9 libraries (stage 1-stage 3) produced over 8 G of clean base, which Q30 percentages (percentage of sequences with sequencing error rates <0.1%) and GC percentages ranging from 92% to 93% and 44% to 46%, respectively (Table S2). All bases were assembled into 282,988 unigenes (longest transcript of each gene) with a mean length of 643 bp (Table S3). KEGG, GO, NR, Swiss prot, TrEMBL and KOG database were used to annotated the predicted protein sequence with an E-value threshold of 1e-5, identity and sequence coverage was more than 30%. Finally, 43,975 (15% of total unigenes) unigenes were annotated by at least one database (Table S4). These data showed that RNA-seq was high quality and could be used for further analysis.

We further studied the changes in gene expression profiles of samples taken during the three kernel developmental stages. Similar to the differential metabolite analysis, we screened the differentially expressed genes (DEGs) under the criteria of $|\log2FC| \geq 1$, and FDR < 0.05. A total of 2469 DEGs, including 1689 up- and 780 down-regulated genes, were identified in stage 2 compared with in stage 1 kernels (Fig. 3B). In the stage 3 vs stage 2 comparison group, 758 genes were up-regulated and 705 genes were down-regulated (Fig. 3C). A total of 267 DEGs were identified among the three comparisons (Fig. 3D). Many DEGs were grouped into various KEGG metabolic pathways. Interesting, "flavonoid biosynthesis" was significantly enriched in stage 1 vs stage 2 and stage 2 vs stage 3 comparison groups (Fig. 3E and F).

3.4. Flavonoids showing different concentrations in the developmental kernels of T. grandis

In total, 124 flavonoids were detected in all the three stages, including 53 flavones, 31 flavonols, 3 proanthocyanidins, 20 flavanones, 9 isoflavones and 8 anthocyanins (Table S1). To identify the flavonoid compounds with differential accumulation among the three

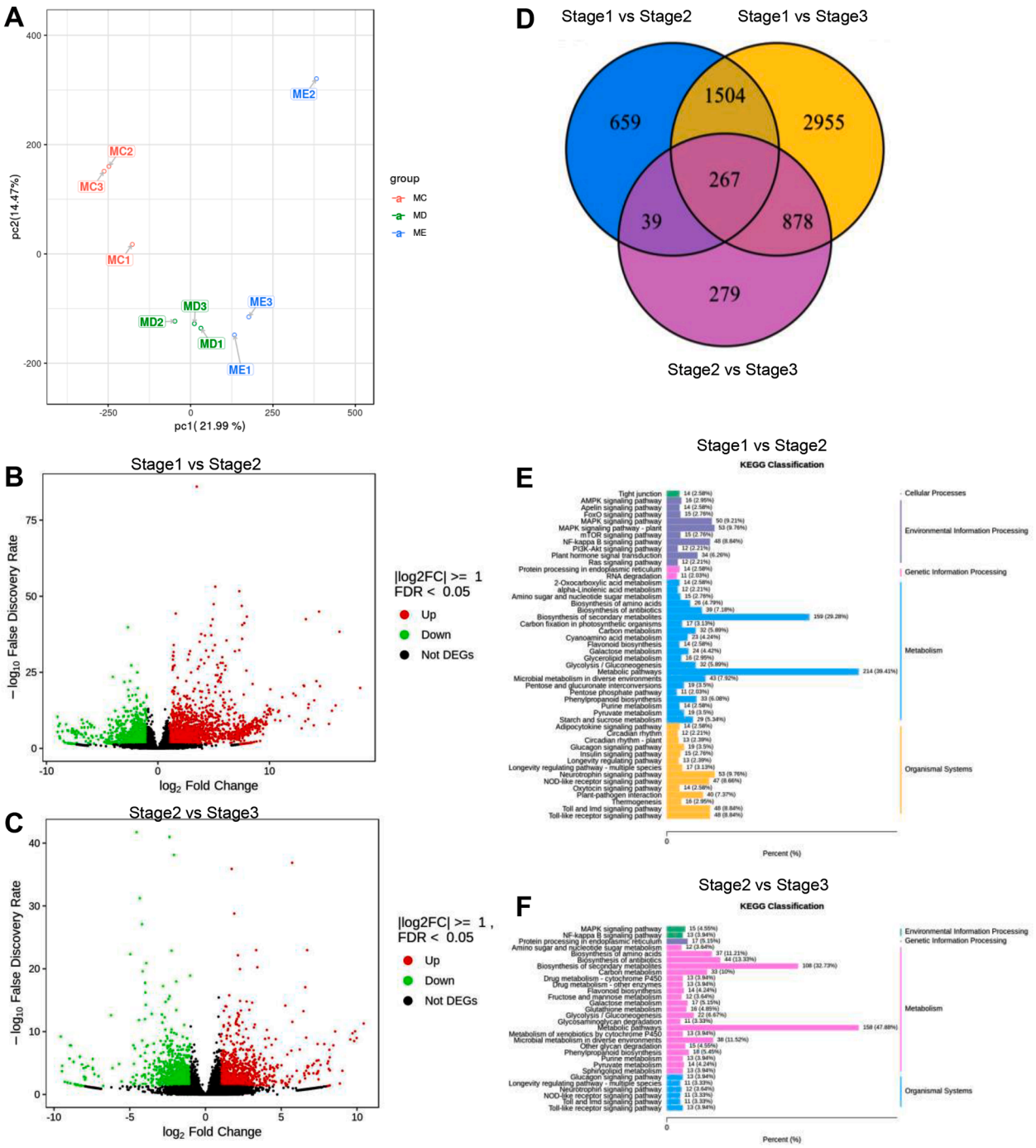

Fig. 3. The statistics of the DEGs in three comparisons. (A) Principal component analysis (PCA) of the genes. MC, MD and ME are the stage1, stage 2 and stage 3, respectively. (B) Volcano plots for DEGs from stage 1 vs stage 2. (C) Volcano plots for DEGs from stage 2 vs stage 3. (D) A venn diagram showed the numbers of the DEGs in three comparisons. (E) KEGG classification of DEGs from stage 1 vs stage 2. (F) KEGG classification of DEGs from stage 2 vs stage 3.

developmental stages of *T. grandis* kernels, the flavonoids from these stages were subjected to a pairwise comparison according to their relative contents. A comparison between stage 1 and stage 2 showed that 26 flavonoids increased and 27 decreased (Fig. 4A), while in the comparison between stage 2 and stage 3, 12 and 18 flavonoids were up-regulated and down-regulated, respectively (Fig. 4B). As the antioxidant activities were stronger in stage 2 stage than stage 1 and stage 3 stages (Fig. 2B and C), flavonoids which down-regulated in stage 1 versus stage 2 and up-regulated in stage 2 versus stage 3 were found (Table S5), including two flavones (butin and chrysoeriol), two flavonols (quercetin 3-O-glucoside and quercetin 4′-O-glucoside), five flavanones (hesperetin, homoeriodictyol, hesperetin 5-O-glucoside, naringenin and naringenin chalcone). Moreover, 4 of the 9 flavonoids (chrysoeriol, quercetin 4′-O-glucoside, hesperetin and homoeriodictyol) were significantly correlated with FRAP or DPPH (Table S5), indicating that they may play important roles in antioxidation in the developmental kernels of *T. grandis*. In order to shed light on the contribution of flavonoids on the total antioxidant activity measured in the kernels, the flavonoid content of *T. grandis* kernels in stage 2 with the highest antioxidant activity was expressed as equivalents of spiraeoside, chrysoeriol, hesperetin, naringenin and rutin, respectively. The results of DPPH radical scavenging activity determination showed that the antioxidant activity

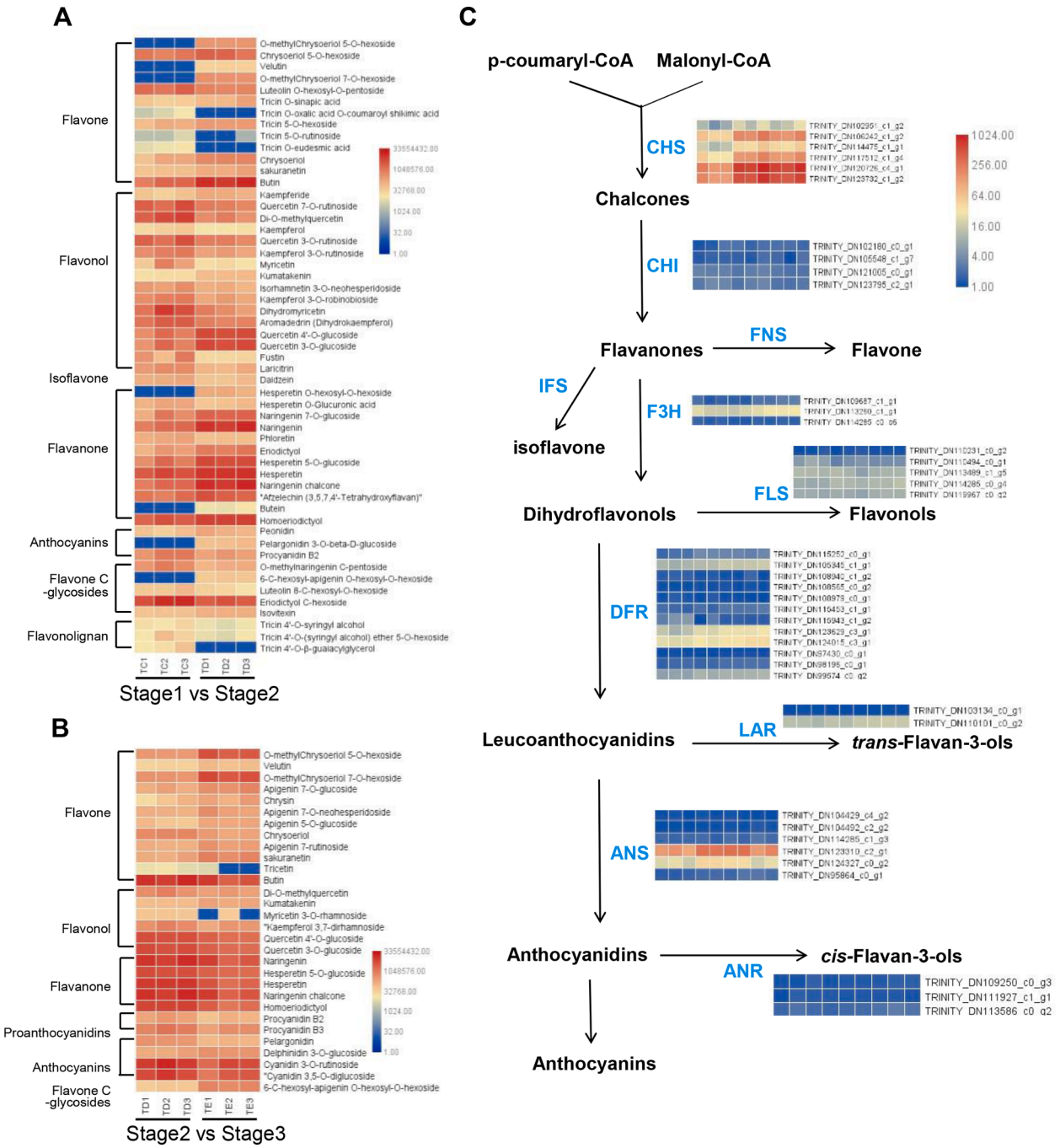

Fig. 4. Differential accumulated flavonids and flavonoid biosynthetic pathway genes analysis. (A) Heatmap of relative content of differential accumulated flavonids in stage 1 vs stage 2. (B) Heatmap of relative content of differential accumulated flavonids in stage 2 vs stage 3. Square on heatmaps represents one of the three repetitions of a *T. grandis* kernel development stage. (C) Biosynthetic pathway of flavonoids. This pathway shows the major flavonoid metabolic intermediates and their synthetases. CHS, chalcone synthase; CHI, chalcone isomerase; F3H, flavanone 3-β-hydroxyalse; IFS, isoflavone synthase; FNS, Flavonoid synthase; FLS, flavonol synthase; DFR, Dihydroflavonol 4-reductase; ANS, anthocyanidin synthase; LAR, leucoanthocyanidin reductase; ANR, anthocyanidin reductase. The heatmaps next to these enzymes are made by FPKM values of unigenes annotated as corresponding gene. Square on heatmaps represents one of the three repetitions of a *T. grandis* kernel development stage.

of spiraeoside, hesperetin and rutin was significantly higher than that of the extracts, and the antioxidant activity of chrysoeriol and naringenin was at least 1/3 higher than that of the extracts. The results indicated that flavonoids contributed greatly to the total antioxidant activity of the extract (Fig. S1).

3.5. Correlation analysis between flavonoid biosynthetic gene expression and flavonoid derivatives

In this study, 41 unigenes that encode enzymes associated with flavonoid biosynthesis were identified based on the enriched KEGG pathways and Gene Ontology function analysis, including 6 CHS genes, 4 CHI genes, 3 F3H genes, 5 FLS genes, 2 LAR genes, 3 ANR genes, 6 ANS gene, 4 IFR genes, and 12 DFR genes (Fig. 4C). Pearson's correlations were performed between the expression of unigenes of flavonoid

biosynthesis pathway and relative content of the nine flavonoids shown in Table S5. The results showed that 2 unigenes for CHS (TRINITY_DN106242_c1_g2 and TRINITY_DN120726_c4_g1), 1 unigene for DFR (TRINITY_DN115252_c0_g1), 2 unigenes for ANS (TRINITY_DN123310_c2_g1 and TRINITY_DN124327_c0_g2) were significantly correlated with at least 7 of the 9 flavonoids, respectively (Fig. 5A), suggesting that these unigenes were key indirect contributors to antioxidant capacity. In addition, in order to find more other genes that may regulate the 4 flavonoids (chrysoeriol, quercetin 4′-O-glucoside, hesperetin and homoeriodictyol) significantly correlated with FRAP or DPPH, Pearson's correlations were performed between all transcriptomic data and these 4 flavonoids. Genes significantly correlated with chrysoeriol, quercetin 4′-O-glucoside, hesperetin or homoeriodictyol with a Pearson's correlation coefficient ≥0.9 were shown in Fig. S2 and Table S6.

3.6. Sequence and phylogenetic analyses of TgDFR1 and TgDFR2

Using the BLAST and ORFfinder tools in NCBI, the coding regions of *TgDFR1* (TRINITY_DN115252_c0_g1_i4) and *TgDFR2* (TRINITY_DN99574_c0_g1_i1) were identified from the sequences of unigenes. The expression of *TgDFR2* was not significantly correlated with flavonoids (here it was used as control). Unfortunately, the length of unigenes annotated as CHS and ANS were too short to obtain complete coding regions. Therefore, only *TgDFR1* and *TgDFR2* were used for subsequent experiments.

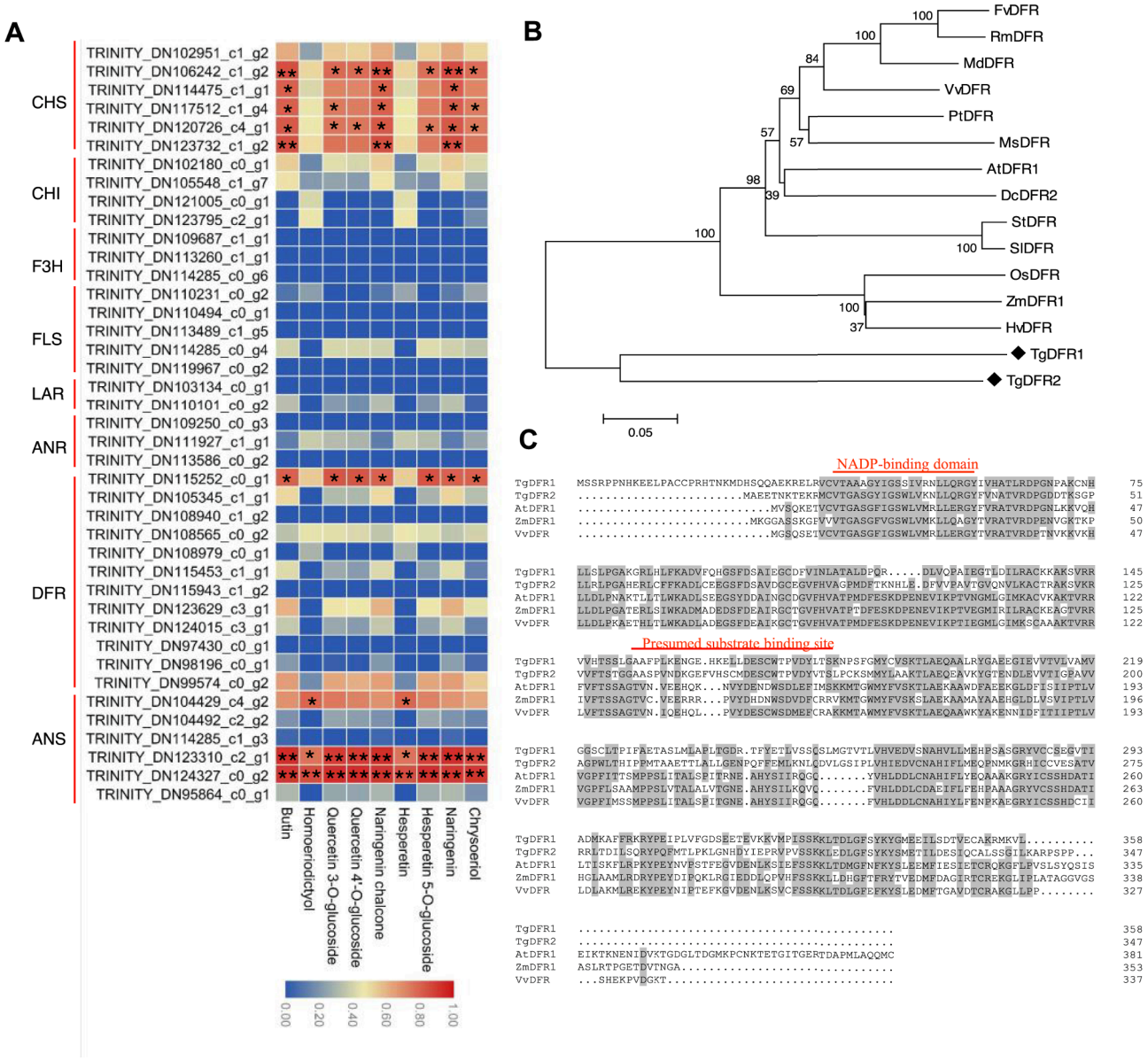

Fig. 5. Flavonoid biosynthesis related unigenes positively correlated with key flavonoids. (A) The heatmap is made by correlation coefficients between FPKM value of flavonoid biosynthetic pathway genes and relative content of 9 flavonoid metabolites listed in Table S5. *, $p < 0.05$, **, $p < 0.01$. (B) Phylogenetic analysis of TgDFR with other DFRs from diverse organisms constructed by the neighbor-joining method based on 1000 bootstrap replicates. (C) Alignment of the deduced amino acid sequences of TgDFR1(TRINITY_DN115252_c0_g1) and TgDFR2(TRINITY_DN99574_c0_g1) along with other DFRs. The GenBank accession numbers of the DFR protein sequences are as follows: *Arabidopsis thaliana* AtDFR (NM_123645), *Dianthus caryophyllus* DcDFR2 (Z67983), *Fragaria vesca* FvDFR (AHL46446), *Hordeum vulgare* HvDFR (S69616), *Malus domestica* MdDFR (NP_001280868), *Medicago sativa* MsDFR (AEI59122), *Oryza sativa* OsDFR (AB003495), *Populus trichocarpa* PtDFR (XP_006383711), *Rosa multiflora* RmDFR (AJT55524), *Solanum tuberosum* StDFR (NP_001274988), *Solanum lycopersicum* SlDFR (NP_001234408), *Vitis vinifera* VvDFR (NP_001268144), *Zea mays* ZmDFR1 (Y16040).

To further investigate the amino acid sequence homology of TgDFR1 and TgDFR2 to other known DFRs, a phylogenetic tree was generated by the neighbor-joining method, and the results showed that DFRs from monocots, dicots and gymnosperms were clearly classified into different branches (Fig. 5B), TgDFR1 and TgDFR2 clustered within a separate subgroup on account of *T. grandis* belongs to gymnosperms (there were no report of DFRs in other gymnosperms), indicating that these two DFR-like proteins might participated in the catalyzing of dihydroflavonols to leucoanthocyanidins in the flavonoid biosynthetic pathway.

Multiple alignment of TgDFR1 and TgDFR2 along with DFRs from other species indicated that *N*-terminus regions of the two DFRs contained putative NADP-binding region which was conserved in all NADPH-dependent reductases (Fig. 5B). DFR proteins was reported to have a substrate-binding region which was composed of 26 amino acid residues such as 131–156 region in grape DFR (Petit et al., 2007; Johnson et al., 2001), while TgDFR1 and TgDFR2 also had some conserved amino acid residues in the corresponding region.

3.7. Overexpression of TgDFR1 in tobacco leaves resulted in increased DPPH activity and FRAP

TgDFR1 and *TgDFR2* were transient expressed in leaves of *N. benthamiana* to verify its function on antioxidant activity. Subcellular localization was observed via confocal laser scanning microscopy, Fig. 6A showed that *TgDFR1* and *TgDFR2* widely expressed in cell membrane and cytoplasm. In order to further validate the performance of TgDFR1 and TgDFR2, tissues used for DPPH radical scavenging activity and FRAP analyses were sampled and tested. The results showed that only TgDFR1 could dramatically increase DPPH activity and FRAP (Fig. 6B).

3.8. Identification of candidate transcription factors involved in flavonoid biosynthesis pathway

Transcription factors are critical to regulate gene expression. To search for the transcription factors that were co-expressed with unigenes for CHS (TRINITY_DN106242_c1_g2 and TRINITY_DN120726_c4_g1), DFR (TRINITY_DN115252_c0_g1) and ANS (TRINITY_DN123310_c2_g1 and TRINITY_DN124327_c0_g2), Pearson's correlation analysis was performed between the expression level of all the transcripts annotated as transcription factors and the candidate genes (Fig. S3A–E). The transcription factors with Pearson's correlation coefficients ≥0.9 were selected. From these selected transcription factors, there are six MYB family (one positive correlation and five negative correlation), seven bHLH family (three positive correlation and four negative correlation), three bZIP family (negative correlation) and eight other family transcription factors may play positive or negative regulatory roles in *T. grandis* kernel (Fig. S3).

3.9. Validation of RNA-seq data using qRT-PCR

To validate the gene expression patterns from RNA-Seq results, 7 genes involved in flavonoid biosynthesis and other 51 genes were randomly selected from RNA-seq data and their transcriptional abundance was detected using qRT-PCR. Primer pairs used were listed in Table S7. As expected, the qRT-PCR and RNA-Seq data were highly correlated with an r of 0.730 ($p < 0.001$), suggesting that the expression data from RNA-seq were reliable (Fig. S4).

4. Discussion

T. grandis seeds have used as traditional medicine for thousands of years in China due to its abundant bioactive components, such as tocopherols, unsaturated fatty acids and flavonoids (Dai et al., 2007; Ding et al., 2020; He et al., 2016; Lou et al., 2019). In this study, we found that flavonoids content of *T. grandis* kernels was increased from 0.423 mg/g to 8.29 mg/g from stage 1 to stage 3 (Fig. 2A), which meaned that *T. grandis* kernels were rich in flavonoids, especially in mature stage 3. However, very little is known about flavonoid composition and the molecular mechanism of flavonoid biosynthesis in *T. grandis* kernels. Previous studies have shown that *T. grandis* seed oils and seed extracts have strong antioxidant activity, but detailed studies on antioxidant substances phenols and flavonoids are rarely reported (Cui et al., 2018). In this study, we performed transcriptome sequencing and metabolomics analysis on the three development stages of *T. grandis* kernels (stage 1, stage 2 and stage 3). A total of 124 flavonoids were detected.

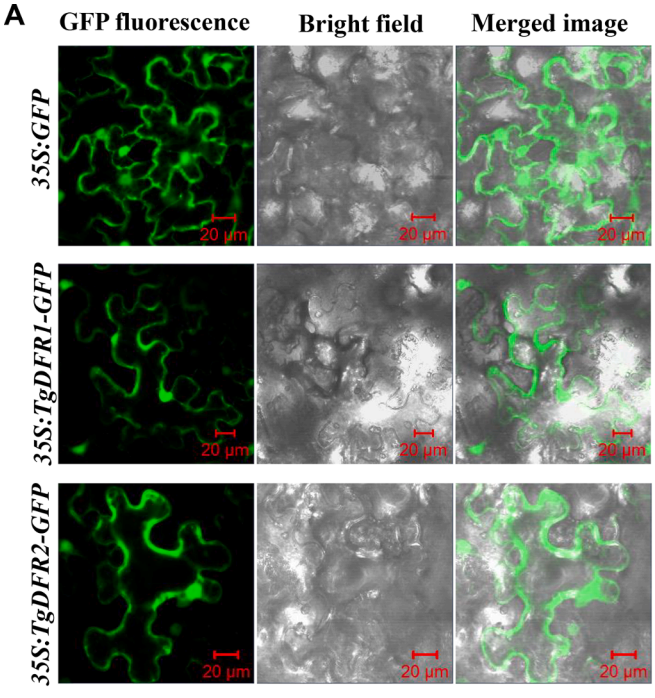

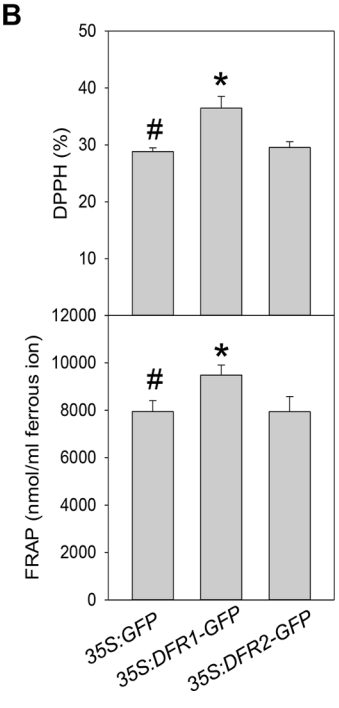

Fig. 6. Overexpression of *TgDFR1* and *TgDFR2* in the leaves of *N. benthamiana*. (A) Subcellular localization of TgDFR1 and TgDFR2. Subcellular localization experiments were conducted with TgDFR1 (middle panel) and TgDFR2 (lower panel) fused GFP as well as with GFP control vector (upper panel). (B) Changes in DPPH radical scavenging activity and FRAP values. TgDFR1 and TgDFR2 fused GFP as well as GFP control vector were transiently expressed in the leaves of *N. benthamiana* for one week. Then DPPH and FRAP were detected in methanol extracts of leaves. Data are means ± SEM (n = 3), asterisk (*) means $p < 0.05$.

Flavones (53) and flavonols (31) were the main components, of which 70 were glycosides, which were similar to those of Tartary buckwheat seeds (Li et al., 2019). It is worth noting that nine isoflavones were also detected in *T. grandis* kernels. According to previous studies, isoflavones mainly exist in legumes, which can not only help legumes to form root nodules (Kosslak et al., 1987), but also act as estrogens to resist cancer (Duffy et al., 2007), indicating that *T. grandis* kernels can also be used as a source of isoflavones.

The antioxidant activities of extracts from *T. grandis* kernels were determined by DPPH and FRAP, respectively. Nine flavonoids related to antioxidant activity were identified by the analysis of differential metabolites in three periods, which were chrysoeriol, naringenin, butin, hesperetin5-O-glucoside, hesperetin, naringenin chalcone, quercetin4′-O-glucoside (spiraeoside), quercetin3-O-glucoside (isotrifoliin), and homoeriodictyol respectively. The main flavonoids in the leaves of *Ginkgo biloba*, which is also a gymnosperm, include quercetin, quercetin-3-O-α-rhamnopyranoside and myricetin-3-O-rhamnopyranoside (Xu et al., 2018). Studies have shown that some of them also have the potential to treat multiple diseases. Hesperetin can prevent neuroinflammation and memory loss by regulating TLR4/NF-κB signal pathway (Ikram et al., 2019; Muhammad et al., 2019). Naringenin and quercetin possess anti-inflammatory and antiallergic activity in mice and have therapeutic potential for sepsis, fulminanthepatitis, fibrosisandcancer caused by inflammation (Escribano-Ferrer et al., 2019; Zeng et al., 2018). Myricitrin can reduce the adverse metabolic reactions of mice fed with long-term high-fat diet, thus showing anti-atherosclerotic and anti-hyperlipidemiceffects (Gao et al., 2019; Kim et al., 2019). This is the first time that flavonoids related to antioxidant activity have been found in *T. grandis* kernels, which deepens our understanding of flavonoid metabolism during *T. grandis* kernel development, and is of great significance for the development of better *T. grandis* seed products.

Through KEGG enrichment analysis and gene functional annotation of transcriptome, some enzyme genes and transcription factors related to flavonoid biosynthesis were found, in which the expression pattern of the unigenes for CHS (TRINITY_DN106242_c1_g2, TRINITY_DN120726_c4_g1 and TRINITY_DN123732_c1_g2), DFR (TRINITY_DN115252_c0_g1) and ANS (TRINITY_DN123310_c2_g1 and TRINITY_DN124327_c0_g2) was significantly related to the 7 differential flavonoid metabolites which have high correlation with antioxidant activity. Further studies showed that overexpression of *TgDFR1* in tobacco leaves could significantly increase DPPH activity and FRAP, suggested that DFR might be related to the change of antioxidant activity during kernel development of *T. grandis*. Previous studies have shown that DFR and CHS play key roles in flavonoid biosynthesis in strawberry (Miosic et al., 2014), apple (Tian et al., 2017), grape (Wang et al., 2016) and many other plants.

Previous studies have identified several transcription factors that positively or negatively regulate flavonoid biosynthesis in plants. For example, overexpression of FtMYB1 and FtMYB2 in *Nicotiana tabacum* accumulated more proanthocyanidins through affecting the expressions of PAL, CHI, F3H, FLS, DFR, and ANS (Bai et al., 2014). It was also found that FtMYB15 and FtWD40 induced the expressions of the early and late flavonoid biosynthesis genes (Luo et al., 2018; Yao et al., 2017). In addition, FtMYB116 was demonstrated to accumulation of rutin by directly regulating the expression of F3H and indirectly regulating the expression of PAL, F3H, FLS and CHS under red and blue light in Tartary buckwheat (Zhang et al., 2019). In contrast, FtMYB3 interacting with FtJAZ2 could repress anthocyanin biosynthesis under cold stress (Luo et al., 2017). In this study, Pearson correlation analysis between transcripts annotated as transcription factors and candidate unigenes revealed that the expression levels of some transcription factors were closely correlated to the flavonoid biosynthesis pathway genes, indicating that these transcription factors may regulate the expression of flavonoid biosynthesis pathway genes and indirectly contribute to flavonoid accumulation in development *T. grandis* kernels. Notably, there are six MYB transcription factors (DN106512_c2_g5, DN112790_c2_g1, DN114418_c4_g3, DN115383_c1_g3, DN117171_c1_g1 and DN97942_c0_g1) were found to be closely correlated to the candidate unigenes for FDR, ANS and CHS. In addition to MYBs, we also found other transcription factors, such as bHLH, HD-ZIP, GATA family members (Fig. S3F), suggesting that these transcription factors may act as new candidate regulators for flavonoid biosynthesis.

5. Conclusions

In summary, transcriptome sequencing and metabolomics analysis were performed to identify key regulators of flavonoid biosynthesis and main contributors for antioxidant activity. It was found that chrysoeriol, naringenin, butin, hesperetin5-O-glucoside, hesperetin, naringenin chalcone, quercetin4′-O-glucoside, quercetin3-O-glucoside, and homoeriodictyol were highly correlated with antioxidant activity, indicating that they are the flavonoid compositions mainly contributing to antioxidant capacity. Further correlation analysis showed that the unigenes for CHS, DFR and ANS significantly correlated with the 9 flavonoids, suggesting that CHS, DFR and ANS play key roles in regulating the 9 flavonoids biosynthesis and further contributed indirectly to antioxidant capacity of *T. grandis* kernels. We further confirmed that overexpressed *TgDFR1* in tobacco leaves resulted in increased antioxidant activity. Moreover, the candidate regulatory genes for flavonoid biosynthesis in development *T. grandis* kernels were also identified via Pearson correlation analysis. These results are helpful for us to better understand the flavonoid biosynthetic pathway in *T. grandis* kernels, and will provide a platform for future molecular biological research and molecular breeding on *T. grandis*.

CRediT authorship contribution statement

Feicui Zhang: Methodology, Validation, Investigation, Resources, Writing – original draft. **Zhenmin Ma:** Methodology, Validation, Investigation. **Yan Qiao:** Methodology, Investigation. **Zhanqi Wang:** Methodology, Investigation. **Wenchao Chen:** Methodology, Validation, Investigation. **Shan Zheng:** Methodology, Investigation. **Chenliang Yu:** Methodology, Software. **Lili Song:** Resources, Writing – review & editing, Supervision. **Heqiang Lou:** Methodology, Writing – review & editing, Supervision. **Jiasheng Wu:** Resources, Supervision, Funding acquisition.

Declaration of Competing Interest

The authors declare that they have no known competing financial interests or personal relationships that could have appeared to influence the work reported in this paper.

Acknowledgements

This work was funded by the National Natural Science Foundation of China (31901339), the Fundamental Research Funds for the Provincial Universities of Zhejiang (2020YQ003), the National Natural Science Foundation of China (31960441), the Key Research and Development Program of Zhejiang Province (2021C02001), the State Key Laboratory of Subtropical Silviculture (ZY20180312 and ZY20180209), the Young Elite Scientists Sponsorship Program by China Academy of Space Technology (CAST) (2018QNRC001), the Open fund of Zhejiang Key Laboratory for Modern Silvicultural Technology (201607).

Appendix A. Supplementary data

Supplementary data to this article can be found online at https://doi.org/10.1016/j.foodchem.2021.131558.

References

Appelhagen, I., Jahns, O., Bartelniewoehner, L., Sagasser, M., Weisshaar, B., & Stracke, R. (2011). Leucoanthocyanidin dioxygenase in *Arabidopsis thaliana*: Characterization of mutant alleles and regulation by MYB–BHLH–TTG1 transcription factor complexes. *Gene, 484*(1-2), 61–68. https://doi.org/10.1016/j.gene.2011.05.031

Bai, Y.-C., Li, C.-L., Zhang, J.-W., Li, S.-J., Luo, X.-P., Yao, H.-P., … Wu, Q.i. (2014). Characterization of two tartary buckwheat R2R3-MYB transcription factors and their regulation of proanthocyanidin biosynthesis. *Physiologia Plantarum, 152*(3), 431–440. https://doi.org/10.1111/ppl.12199

Benzie, I. F. F., & Strain, J. J. (1996). The ferric reducing ability of plasma (FRAP) as a measure of 'antioxidant power': The FRAP assay. *Analytical Biochemistry, 239*(1), 70–76. https://doi.org/10.1006/abio.1996.0292

Bonvehí, J. S., Torrentó, M. S., & Lorente, E. S. (2001). Evaluation of polyphenolic and flavonoid compounds in honey-bee collected pollen produced in Spain. *Journal of Agricultural and Food Chemistry, 49*(4), 1848–1853. https://doi.org/10.1021/jf0012300

Cui, H. X., Duan, F. F., Jia, S. S., Cheng, F. R., & Yuan, K. (2018). Antioxidant and Tyrosinase Inhibitory Activities of Seed Oils from *Torreya grandis* Fort. ex Lindl. *Biomed Research International, 2018*, 5314320. https://doi.org/10.1155/2018/5314320.

Dai, R., Jiang, D., Li, W., Zhang, Y., Yu, Y., Deng, Y., & Meng, W. (2007). The determination of the total flavonoids by UV and a flavone glycoside by HPLC in *Torreya grandis* Fort Leaves. *IEEE/ICME International Conference on Complex Medical Engineering, 1887–1891*. https://doi.org/10.1109/ICCME.2007.4382076

Ding, M., Lou, H., Chen, W., Zhou, Y., Zhang, Z., Xiao, M., … Song, L. (2020). Comparative transcriptome analysis of the genes involved in lipid biosynthesis pathway and regulation of oil body formation in *Torreya grandis* kernels. *Industrial Crops and Products, 145*, 112051. https://doi.org/10.1016/j.indcrop.2019.112051

Duffy, C., Perez, K., & Partridge, A. (2007). Implications of phytoestrogen intake for breast cancer. *CA-A Cancer Journal for Clinicians, 57*(5), 260–277. https://doi.org/10.3322/CA.57.5.260

Escribano-Ferrer, E., Queralt Regué, J., Garcia-Sala, X., Boix Montañés, A., & Lamuela-Raventos, R. M. (2019). *In vivo* anti-inflammatory and antiallergic activity of pure naringenin, naringenin chalcone, and quercetin in mice. *Journal of Natural Products, 82*(2), 177–182. https://doi.org/10.1021/acs.jnatprod.8b00366

Gao, J., Liu, C. C., Zhang, H. P., Sun, Z., & Wang, R. M. (2019). Myricitrin exhibits anti-atherosclerotic and anti-hyperlipidemic effects in diet-induced hypercholesterolemic rats. *AMB Express, 9*, 204. https://doi.org/10.1186/s13568-019-0924-0

Giménez-Bastida, J. A., & Zieliński, H. (2015). Buckwheat as a functional food and its effects on health. *Journal of Agricultural and Food Chemistry, 63*(36), 7896–7913. https://doi.org/10.1021/acs.jafc.5b02498

Harborne, J. B., & Williams, C. A. (2000). Advances in flavonoid research since 1992. *Phytochemistry, 55*(6), 481–504. https://doi.org/10.1016/S0031-9422(00)00235-1

He, Z., Zhu, H., Li, W., Zeng, M., Wu, S., Chen, S., … Chen, J. (2016). Chemical components of cold pressed kernel oils from different *Torreya grandis* cultivars. *Food Chemistry, 209*, 196–202. https://doi.org/10.1016/j.foodchem.2016.04.053

Hu, Y., Hou, Z., Liu, D., & Yang, X. (2016). Tartary buckwheat flavonoids protect hepatic cells against high glucose-induced oxidative stress and insulin resistance via MAPK signaling pathways. *Food & Function, 7*(3), 1523–1536. https://doi.org/10.1039/C5FO01467K

Hu, Y., Zhao, Y., Yuan, L., & Yang, X. (2015). Protective effects of tartary buckwheat flavonoids on high TMAO diet-induced vascular dysfunction and liver injury in mice. *Food & Function, 6*(10), 3359–3372. https://doi.org/10.1039/C5FO00581G

Ikram, M., Muhammad, T., Rehman, S. U., Khan, A., Jo, M. G., Ali, T., & Kim, M. O. (2019). Hesperetin confers neuroprotection by regulating Nrf2/TLR4/NF-κB signaling in an Aβ mouse model. *Molecular Neurobiology, 56*(9), 6293–6309. https://doi.org/10.1007/s12035-019-1512-7

Johnson, E. T., Ryu, S., Yi, H., Shin, B., Cheong, H., & Choi, G. (2001). Alteration of a single amino acid changes the substrate specifificity of dihydroflavonol 4-reductase. *Plant Journal, 25*, 325–333. https://doi.org/10.1046/j.1365-313x.2001.00962.x

Kim, Y.-J., Kim, S. R., Kim, D. Y., Woo, J. T., Kwon, E.-Y., Han, Y., … Jung, U. J. (2019). Supplementation of the flavonoid myricitrin attenuates the adverse metabolic effects of long-term consumption of a high-fat diet in mice. *Journal of Medicinal Food, 22*(11), 1151–1158. https://doi.org/10.1089/jmf.2018.4341

Kosslak, R. M., Bookland, R., Barkei, J., Paaren, H. E., & Appelbaum, E. R. (1987). Induction of *Bradyrhizobium japonicum* common nod genes by isoflflavones isolated from *Glycine max*. *Proceedings of the National Academy of Sciences of the United States of America, 84*, 7428–7432. https://doi.org/10.1073/pnas.84.21.7428

Lee, C. C., Shen, S. R., Lai, Y. J., & Wu, S. C. (2013). Rutin and quercetin, bioactive compounds from tartary buckwheat, prevent liver inflammatory injury. *Food & Function, 4*, 794–802. https://doi.org/10.1039/C3FO30389F

Lepiniec, L., Debeaujon, I., Routaboul, J.-M., Baudry, A., Pourcel, L., Nesi, N., & Caboche, M. (2006). Genetics and biochemistry of seed flavonoids. *Annual Review of Plant Biology, 57*(1), 405–430. https://doi.org/10.1146/annurev.arplant.57.032905.105252

Li, H., Lv, Q., Ma, C., Qu, J., Cai, F., Deng, J., … Chen, Q. (2019). Metabolite profiling and transcriptome analyses provide insights into the flavonoid biosynthesis in the developing seed of Tartary Buckwheat (*Fagopyrum tataricum*). *Journal of Agricultural and Food Chemistry, 67*(40), 11262–11276. https://doi.org/10.1021/acs.jafc.9b03135

Li, N., Liu, J.-H., Zhang, J., & Yu, B.-Y. (2008). Comparative evaluation of cytotoxicity and antioxidative activity of 20 flavonoids. *Journal of Agricultural and Food Chemistry, 56*(10), 3876–3883. https://doi.org/10.1021/jf073520n

Liu, M., Veryser, C., Lu, J. G., Wenseleers, T., De Borggraeve, W. M., Jiang, Z. H., & Luyten, W. (2018). Bioassay-guided isolation of active substances from Semen Torreyae identifies two new anthelmintic compounds with novel mechanism of action. *Journal of Ethnopharmacology, 224*, 421–428. https://doi.org/10.1016/j.jep.2018.06.026

Lou, H., Ding, M., Wu, J., Zhang, F., Chen, W., Yang, Y.i., … Song, L. (2019). Full-length transcriptome analysis of the genes involved in tocopherol biosynthesis in *Torreya grandis*. *Journal of Agricultural and Food Chemistry, 67*(7), 1877–1888. https://doi.org/10.1021/acs.jafc.8b06138

Lu, H., Zheng, H., Lou, H., Jiang, L., Chen, Y., & Fang, S. (2010). Using neural networks to estimate the losses of ascorbic acid, total phenols, flavonoid and antioxidant activity in asparagus during thermal treatments. *Journal of Agricultural and Food Chemistry, 58*(5), 2995–3001. https://doi.org/10.1021/jf903655a

Luo, X. P., Li, S. J., Yao, P. F., Li, C. L., Chen, H., Wu, Q., & Zhao, H. X. (2017). The jasmonate-ZIM domain protein FtJAZ2 interacts with the R2R3-MYB transcription factor FtMYB3 to affect anthocyanin biosynthesis in tartary buckwheat. *Turkish Journal of Biology, 41*, 526–534. https://doi.org/10.3906/biy-1610-6

Luo, X., Zhao, H., Yao, P., Li, Q., Huang, Y., Li, C., … Wu, Q.i. (2018). An R2R3-MYB transcription factor FtMYB15 involved in the synthesis of anthocyanin and proanthocyanidins from tartary buckwheat. *Journal of Plant Growth Regulation, 37*(1), 76–84. https://doi.org/10.1007/s00344-017-9709-3

Miosic, S., Thill, J., Milosevic, M., Gosch, C., Pober, S., Molitor, C., … Strack, S. (2014). Dihydroflavonol 4-reductase genes encode enzymes with contrasting substrate specificity and show divergent gene expression profiles in fragaria species. *PLoS One, 9*(11), e112707. https://doi.org/10.1371/journal.pone.0112707

Muhammad, T., Ikram, M., Ullah, R., Rehman, S. U., & Kim, M. O. (2019). Hesperetin, a citrus flavonoid, attenuates LPS-induced neuroinflammation, apoptosis and memory impairments by modulating TLR4/NF-κB signaling. *Nutrients, 11*, 648. https://doi.org/10.3390/nu11030648

Nijveldt, R. J., Nood, E. V., Hoorn, D. E. V., Boelens, P. G., Norren, K. V., & Leeuwen, P. A. V. (2001). Flavonoids: A review of probable mechanisms of action and potential applications. *American Journal of Clinical Nutrition, 74*, 418–425. https://doi.org/10.1093/ajcn/74.4.418

Petit, P., Granier, T., d'Estaintot, B. L., Manigand, C., Bathany, K., Schmitter, J.-M., … Gallois, B. (2007). Crystal structure of grape dihydroflavonol 4-reductase, a key enzyme in flavonoid biosynthesis. *Journal of Molecular Biology, 368*(5), 1345–1357. https://doi.org/10.1016/j.jmb.2007.02.088

Saeed, M. K., Deng, Y., Dai, R., Li, W., Yu, Y., & Iqbal, Z. (2010). Appraisal of antinociceptive and anti-inflammatory potential of extract and fractions from the leaves of *Torreya grandis* Fort Ex. *Lindl. Journal of Ethnopharmacology, 127*(2), 414–418. https://doi.org/10.1016/j.jep.2009.10.024

Tian, J., Chen, M. C., Zhang, J., Li, K. T., Song, T. T., Zhang, X., & Yao, Y. C. (2017). Characteristics of dihydroflavonol 4-reductase gene promoters from different leaf colored *Malus Crabapple* Cultivars. *Horticulture Research, 13*, 17070. https://doi.org/10.1038/hortres.2017.70

Wang, H., Wang, W., Zhan, J., Yan, A., Sun, L., Zhang, G., … Xu, H. (2016). The accumulation and localization of chalcone synthase in grapevine (*Vitis Vinifera L.*). *Plant Physiology and Biochemistry, 106*, 165–176. https://doi.org/10.1016/j.plaphy.2016.04.042

Xu, W., Grain, D., Bobet, S., Gourrierec, J. G., Thevenin, J., Kelemen, Z., … Dubos, C. (2014). Complexity and robustness of the flavonoid transcriptional regulatory network revealed by comprehensive analyses of MYB–bHLH–WDR complexes and their targets in Arabidopsis seed. *New Phytologist, 202*, 132–144. https://doi.org/10.1111/nph.12620

Xu, Y., Tao, Z., Jin, Y., Yuan, Y., Dong, T. T. X., Tsim, K. W. K., & Zhou, Z. (2018). Flavonoids, a potential new insight of *Leucaena leucocephala* foliage in ruminant health. *Journal of Agricultural and Food Chemistry, 66*(29), 7616–7626. https://doi.org/10.1021/acs.jafc.8b02739

Yao, P., Zhao, H., Luo, X., Gao, F., Li, C., Yao, H., … Wu, Q. (2017). *Fagopyrum tataricum* FtWD40 functions as a positive regulator of anthocyanin biosynthesis in transgenic tobacco. *Journal of Plant Growth Regulation, 36*(3), 755–765. https://doi.org/10.1007/s00344-017-9678-6

Zeng, W. F., Jin, L. T., Zhang, F. Y., Zhang, C. L., & Liang, W. (2018). Naringenin as a potential immunomodulator in therapeutics. *Pharmacological Research, 135*, 122–126. https://doi.org/10.1016/j.phrs.2018.08.002

Zhang, D., Jiang, C., Huang, C., Wen, D., Lu, J., Chen, S., … Chen, S. (2019). The light-induced transcription factor FtMYB116 promotes accumulation of rutin in *Fagopyrum tataricum*. *Plant Cell and Environment, 42*, 1340–1351. https://doi.org/10.1111/pce.13470